Ultrastructural localization of chitin in cell walls of *Rigidoporus lignosus,* the white-rot fungus of rubber tree roots

MICHEL R. NICOLE and NICOLE BENHAMOU†

Forestry Canada, Quebec Region, 1055 du PEPS, G1V 4C7 Sainte-Foy, Quebec, Canada; † *Département de Phytologie, Faculté des Sciences de l'Agriculture et de l'Alimentation, Université Laval, G1K 7P4 Sainte-Foy, Quebec, Canada*

The distribution of *N*-acetylglucosamine residues in the cell wall of the white-rot pathogenic fungus, *Rigidoporus lignosus*, was studied by using gold labelled wheatgerm agglutinin bound to ovomucoid-colloidal gold. Ultrastructural investigation of *R. lignosus*-infected root tissues of *Hevea brasiliensis* showed a modification of the fungal cell wall throughout the infection process. Gold particles were found to occur on both thick- and thin-walled hyphae of *R. lignosus* rhizomorphs at the root surface. Walls of hyphae that had penetrated the roots were only labelled when they were out of the host cell, suggesting that modification of chitin molecules may be related to the excretion of host cell wall degrading enzymes. Variation in the distribution of gold particles was observed over hyphal walls of both colonized phellem and xylem cells. The observation that *N*-acetylglucosamine residues were released in the host cell cytoplasm suggests that lytic enzymes alter the fungal cell walls. Released chitin oligosaccharides may play a role in the induction of the root's defence system against fungal attack.

INTRODUCTION

In tropical areas, *Hevea brasiliensis* Kunth Muell. Arg., is cultivated for the production of rubber from the latex synthesized in phloem laticifers. Of several rubber tree pathogens that have been identified in plantations [*10*], root rot fungi are the commonest causes of disease recorded in west Africa [*27*]. One of the main damaging root decaying fungi is a basidiomycete, *Rigidoporus lignosus* (Klotzsch) Imazeki, that causes a white-rot of host tissues. It attacks roots by means of fast growing rhizomorphs which contain both thick- and thin-walled mycelium. *R. lignosus* rhizomorphs have been demonstrated to produce specialized infection hyphae that are able to undergo considerable physiological changes in relation to excretion of enzymes degrading host cells [*16*]. Such infective hyphae penetrate roots *via* natural openings, wounds, or after fungal-induced cell wall degradation [*30, 32*].

Extensive root tissue colonization by *R. lignosus* results in severe cell damage

probably due to the activity of fungal enzymes secreted during infection [*18, 19*]. These enzymes are thought to be involved in the decay process by altering suberized, cellulosic and lignified root cell walls as suggested by previous ultrastructural observations [*29, 30, 32*].

Although these studies have contributed to our understanding of different aspects of the interaction between rubber tree root tissues and *R. lignosus*, to our knowledge there has been no report dealing with the modifications of fungal cell walls during pathogenesis. Chitin, a β-(1,4)-linked homopolymer of *N*-acetyl-D-glucosamine (GlcNAc), and β-(1,3/1,6)-D-glucans are known to be ubiquitous components of walls of higher fungi [*3, 22, 42, 43*]. Chitin in fungi can be detected by chemical methods [*11, 37, 40*] and by cytochemical techniques using either chitinase–gold complexes [*9*] or the wheatgerm agglutinin (WGA) which binds strongly to GlcNAc residues [*4, 36*]. The use of WGA in conjunction with colloidal gold has demonstrated the localization of GlcNAc within cell walls of different plant pathogenic fungi such as rust fungi [*21*], the bean anthracnose fungus [*35*], vascular disease-causing fungi [*3*] and scleroderris canker agents [*6*]. Chitin localization was also recently found helpful for studying (i) the apical growth of filamentous fungi [*13*], (ii) the wall architecture in mycorrhizal fungi [*8, 20*], and (iii) antagonistic interactions between *Trichoderma* sp. and *Fusarium* spp. [*12*].

Although several authors have investigated the chemical composition of the cell walls of several basidiomycetes [*11, 22, 42, 43*], little attention has been paid to the distribution of chitin within cell walls of lignin-decaying fungi. The present paper reports the distribution of chitin in the cell walls of the root rotting fungus, *R. lignosus*, during the infection process of rubber trees using the WGA–ovomucoid gold method. Particular attention was given to morphological changes of fungal walls which occur during young root penetration and colonization.

MATERIALS AND METHODS

Fungal culture and growth conditions
Isolates of *R. lignosus* were collected in rubber tree plantations in the Ivory Coast. The mycelium was obtained by growing *R. lignosus*, strain 1, on a 2 % malt agar medium (Difco Lab., Detroit, Michigan) at 28 °C.

Artificial inoculations of plant material
Seeds of rubber trees, clone GT 1, were collected in a plantation of the Institut de Recherche du Caoutchouc of Ivory Coast (IRCA). After germination in sand, young seedlings were transferred to tubs (1 × 1 × 1 m) filled with forest soil. A high moisture level, maintained in the soil by daily watering to saturation, was monitored with a neutronic moisture gauge (Solo 20, Nardeux, France). Seedling inoculation was performed as described previously [*26*]. Briefly, five pre-infected rubber wood fragments were placed against the tap root of each 1-month old seedling, 20 cm deep in the soil. Root samples were collected at varying intervals following inoculation. Non-infected plants were used as controls.

Preparation of samples for electron microscopy

Infected roots were fixed *in toto*, for 1 h, in 3 % glutaraldehyde (v/v) (EM grade, Sigma Chemical Co., St Louis, Missouri) in 0·1 M sodium cacodylate buffer, pH 7·2. Small root fragments were then excised and fixed again for 1 h with glutaraldehyde, postfixed with 1 % aqueous osmium tetroxide (EM grade, Sigma) for 1 h at 4 °C, washed in sodium cacodylate buffer before dehydration in a graded series of ethanol, and embedded in Epon 812 or in Araldite. Ultrathin sections, collected on formvar-coated nickel grids (200 mesh) (JBEM Chemical Co., Pointe Claire, Canada), were processed for cytochemical labelling. Observations were carried out with a JEOL 1200 EX electron microscope operating at 80 kV.

For each step of the infection process, several samples per infected plant were treated for TEM. Samples from healthy rubber tree roots were processed as mentioned above and used as controls.

Cytochemical labelling of N-*acetylglucosamine residues* (*chitin*)

The colloidal gold suspension was prepared as described by Grandmaison *et al.* [20]. Because of its low molecular weight, WGA could not be directly complexed to gold. This lectin was used in an indirect labelling procedure for studying the distribution of chitin within cell walls of *R. lignosus* infecting roots of rubber trees. The ovomucoid (Sigma) was chosen as a second-step reagent due to its selective affinity for the WGA [4] and it was complexed to colloidal gold at pH 5·4. Colloidal gold with a mean particle diameter of approx. 15 nm was prepared according to Frens [15].

For indirect labelling, sections of infected or healthy rubber tree roots were first incubated in a drop of WGA [25 µg ml^{-1} in 0·1 M phosphate buffered saline (PBS), pH 7·4] (Sigma) for 30 min at room temperature, rinsed with PBS and then transferred onto a drop of ovomucoid–gold complex for 30 min at room temperature in a moist chamber. They were then thoroughly washed with PBS, rinsed with distilled water and finally contrasted with uranyl acetate and lead citrate before examination.

Specificity of labelling was assessed by means of the following controls: (a) incubation with WGA after preadsorbing the tissues in N-N'-N''-triacetyl chitotriose (Sigma), 3 mg ml^{-1} in PBS; (b) incubation with WGA, followed by unlabelled ovomucoid, and finally the ovomucoid–gold complex; (c) direct incubation with the ovomucoid–gold complex without treatment with the WGA.

Quantification of labelling

The density of labelling over cell walls of healthy root tissues and of *R. lignosus* during the infection process was compared by determining the number of gold particles per square micrometre. Area (Sa) determinations and number of gold particles (Ns) were carried out on scanned micrographs with Image Analyst 7·22 (Automatix, licence number 1596), a picture processing software, loaded on a Macintosh II computer (Apple). The density of labelling (D) was calculated as follows; $D = Ns/Sa$. Density was determined by treating 6–15 micrographs for each estimation.
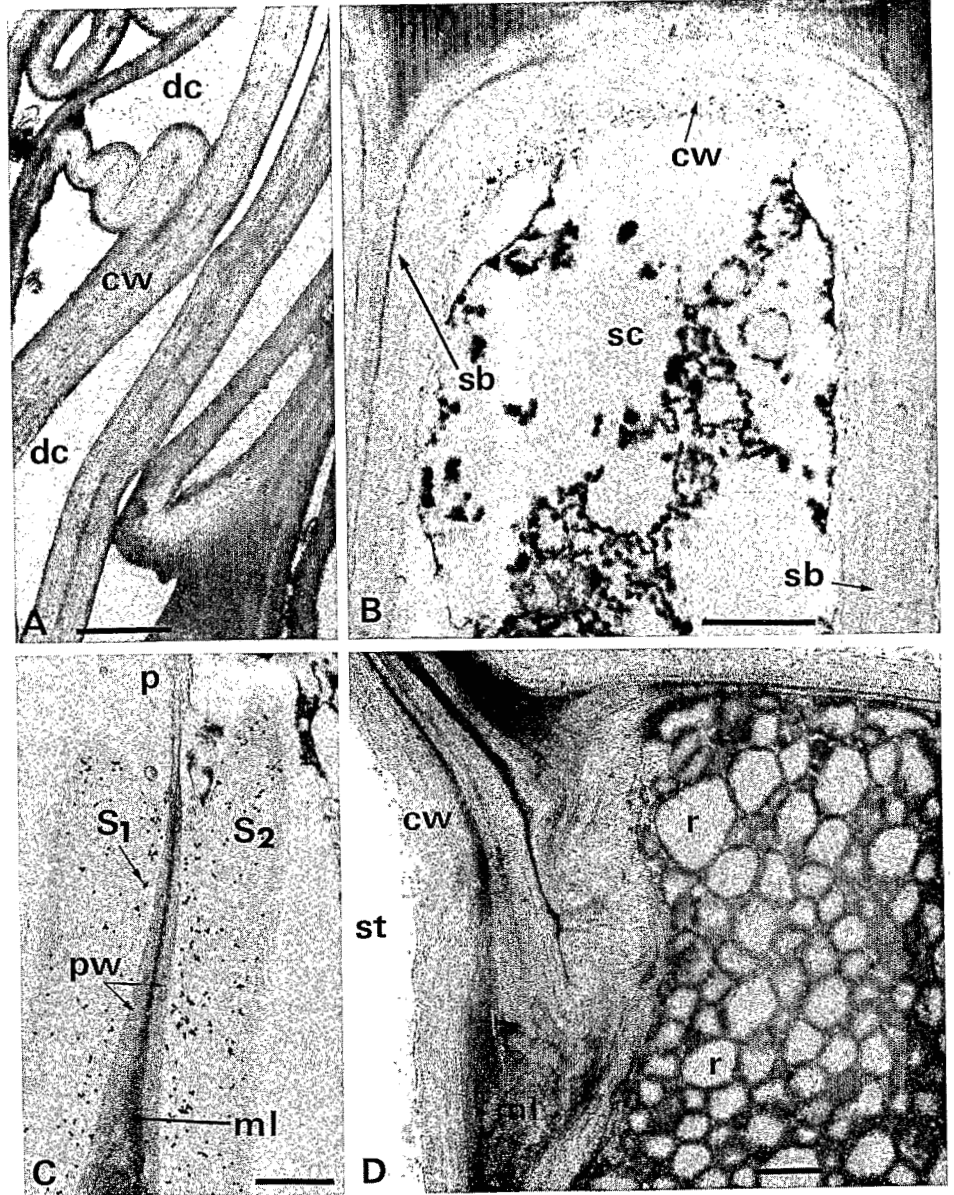
FIG. 1. Transmission electron micrographs of healthy rubber tree roots double-fixed with glutaraldehyde and osmium tetroxide. Sections were treated with the WGA–ovomucoid–gold complex. (A) Primary walls (cw) of dead surface cells (dc) are free of gold particles. Bar = 1 μm. (B) Suberized cells (sc) of the phellem in a young root. Labelling occurs over cellulosic layers of walls (cw). The middle lamella and suberized layers of walls (sb) are free of gold particles. Bar = 1 μm. (C) Walls of xylem cells. Gold granules are distributed mainly over the S1 and S2 layers of secondary walls. Few gold particles are observed over primary walls (pw) and the middle lamella (ml) of xylem elements. p, Pit area. Bar = 1 μm. (D) Walls (cw) of phloem laticifer and sieve tube (st), as well as the middle lamella (ml) do not exhibit any labelling after the treatment with the gold complex. r, Latex particle. Bar = 0·5 μm.

RESULTS

Labelling pattern observed in healthy roots
Following incubation of ultrathin sections of non-inoculated young root tissues with the WGA–ovomucoid–gold complex, variation of labelling was observed over walls of root cells. Primary walls such as dead surface cell walls of the rhytidome exhibited very few gold particles [Fig. 1(A), Table 1]. In the phellem, the outermost wall layers adjacent to the middle lamella, known to be highly suberized, was nearly unlabelled, whereas the non-suberized innermost layers were regularly labelled, especially in areas close to the cell lumina [Fig. 1(B), Table 1]. No gold particles were associated with the middle lamella adjacent to phellem cells. Similarly, very low labelling occurred over walls of phloem cells such as sieve tubes and laticifers [Fig. 1(D), Table 1]. In the xylem,

TABLE 1.

Density of labelling[a] obtained with WGA–ovomucoid–gold complex over cell walls and middle lamellae of rubber root tissues

Rubber root tissue	Fungal localization	Labelling density
Xylem[b]	Secondary cell wall	66.58 ± 29.25
	Primary cell wall	8.45 ± 5.59
	Middle lamella	43.71 ± 14.24
Phloem[b]	Cell wall	2.17 ± 1.88
	Middle lamella	0.00 ± 0.00
Phellem cell walls[b]	Cellulose layer	70.87 ± 15.85
	Suberized layer	4.76 ± 6.87
	Middle lamella	0.00 ± 0.00
Dead surface cell walls[b]		1.94 ± 1.74
Additional cell wall layers in xylem elements[c]		0.47 ± 0.54

[a]Density of labelling is expressed by the number of gold particles $\mu m^{-2} \pm SD$.
[b]In healthy roots.
[c]In infected roots.

secondary cell walls and the electron-opaque middle lamella were labelled [Fig. 1(C), Table 1], whereas pit membranes and primary walls were slightly labelled. All other structures including organelles, cytoplasm and plasma membranes were free of any significant labelling.

Ultrastructural features of infected H. brasiliensis *root tissues*
In agreement with previous reports [*18, 19, 29, 30, 32*], the present observations showed that rhizomorphs of *R. lignosus* grew along tap-roots [Figs 2(D) and 3(A)], and differentiated infectious hyphae that penetrated the outer root tissue through lenticels, wounds and/or after cell wall degradation [Fig. 3(A) and (B)]. During this early stage of root infection, cell walls of hyphae underwent considerable morphological changes since only thin-walled hyphae penetrated the root tissues [Fig. 3(B)]. Pathogen ingress of the rhytidome (= outer bark made of an accumulation of dead cells on the root
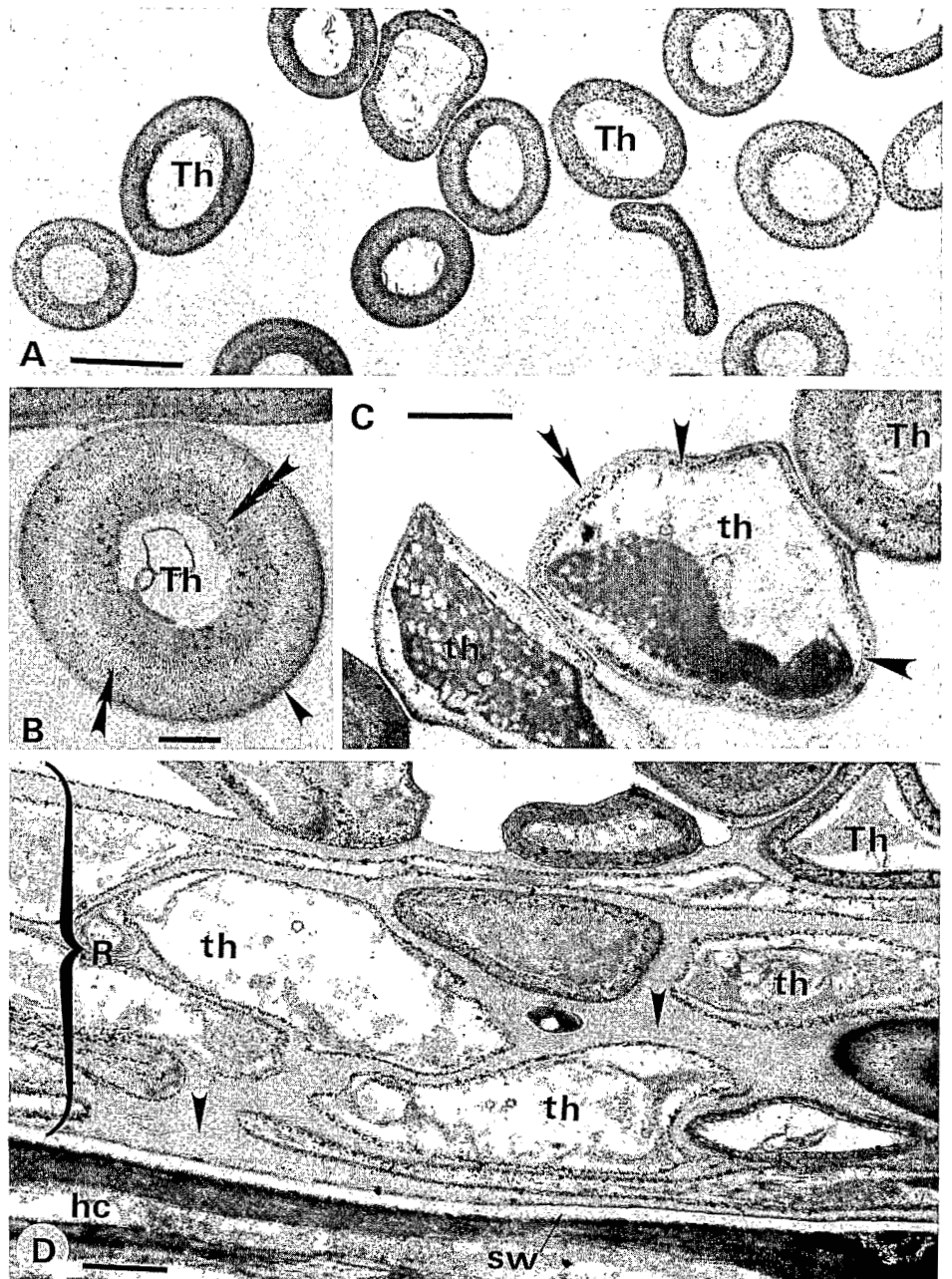
FIG. 2. Transmission electron micrographs of *Rigidoporus lignosus* rhizomorphs in contact with rubber tree roots double-fixed with glutaraldehyde and osmium tetroxide. Sections were treated with the WGA–ovomucoid–gold complex. (A) Cross section in the outermost part of *R. lignosus* rhizomorphs showing labelled thick-walled hyphae (Th). Bar = 2 μm. (B) The internal layer of walls of thick-walled hyphae (Th) is heavily labelled (triple arrowhead), while gold particles are less abundant over the intermediate reticulated layer (double arrowhead). Note there are few gold particles over the external layer of walls (arrowhead). Bar = 0·5 μm. (C) Thin-walled hyphae (th) in *R. lignosus* rhizomorphs. Gold particles are preferentially associated with the innermost wall

surface [*14*]) proceeded by both inter- and intracellular modes of growth. In roots where dead surface cells were apparently missing, hyphae were closely appressed against the outermost cell layer of the phellem and were capable of growing intramurally. Colonization of the vascular stele, occurred *via* infection of parenchyma rays. Although phloem wall degradation was observed in all cell types, hyphae were seldom seen in sieve tubes and were never found in latice vessels. In contrast, xylem cells were intensively colonized. Invasion of these cells proceeded often directly through the middle lamella and pit membrane [Fig. 5(D)]. Degradation of lignified secondary walls was also noticeable and appeared to result from the sequential alteration of the S1, S2 and S3 layers.

Labelling pattern observed in infected roots

Labelling with WGA–ovomucoid–gold complex was performed on sections corresponding to different stages of root infection.

R. lignosus rhizomorphs contained two types of hyphae: thick-walled hyphae mainly distributed in the outermost part of rhizomorphs [Fig. 2(A)] and thin-walled hyphae mainly localized in close contact with the root surface [Fig. 2(D)]. After incubation of sections showing the host–pathogen interface with the gold-complexed probe, it appeared that fungal walls of both types of hyphae were intensely labelled. Gold particles accumulated preferentially over the internal electron-opaque wall layer of thick-walled hyphae [Fig. 2(B), triple arrowhead; Table 2], whereas they were more unevenly distributed over the intermediate reticulated layer [Fig. 2(B), double arrowhead] and over the external fungal wall layer [Fig. 2(B), arrowhead, Table 2].

Thin walled-hyphae apparently formed a pseudosclerenchymatous structure closely appressed to the root surface [Fig. 2(D), 3(A)]. Gold particles were mainly associated with the innermost wall layer [Fig. 2(C)]. Cytoplasm and organelles, including nucleus and mitochondria, as well as the interhyphal-connecting material [Fig. 2(D), arrowheads] were free of labelling.

Incubation with the WGA–ovomucoid–gold complex showed that labelling was less intense over the wall of the hyphal portion actively involved in dead surface cell wall penetration [Fig. 3(B), arrows; Table 2] than in walls of rhizomorph-included hyphae close to the root surface [Fig. 3(B), double arrowheads; Table 2]. However, numerous gold particles were observed over wall hyphal portions which had penetrated host cells [Fig. 3(B), double arrows].

In phellem cells showing the degradation of the suberized wall, labelling was less intense over wall portions in the channel of fungal penetration [Fig. 3(C) arrowheads; Table 2]. Gold particles were abundant at the tip of penetrating hyphae [Fig. 3(C), double arrowheads]. Variation in the distribution of gold particles was observed within hyphae colonizing phellem cells [Figs 3(C), 4(A), 4(B), 4(C); Table 2]. In altered hyphae, gold particles were found around or inside the fungus [Fig. 4(A)] as well as

layers of fungal walls (arrowheads). Labelling does not occur over external wall layers (double arrowhead). Th, Thick-walled hypha. Bar = 1 μm. (D) Interface between *R. lignosus* rhizomorph (R) and the rubber tree root surface. Note that only thin-walled hyphae (th) are in close contact with external root cells (hc). The interhyphal connecting material (arrowheads) is free of gold labelling. Th, Thick-walled hypha; sw, suberized wall. Bar = 1 μm.

surface [*14*]) proceeded by both inter- and intracellular modes of growth. In roots where dead surface cells were apparently missing, hyphae were closely appressed against the outermost cell layer of the phellem and were capable of growing intramurally. Colonization of the vascular stele, occurred *via* infection of parenchyma rays. Although phloem wall degradation was observed in all cell types, hyphae were seldom seen in sieve tubes and were never found in latice vessels. In contrast, xylem cells were intensively colonized. Invasion of these cells proceeded often directly through the middle lamella and pit membrane [Fig. 5(D)]. Degradation of lignified secondary walls was also noticeable and appeared to result from the sequential alteration of the S1, S2 and S3 layers.

Labelling pattern observed in infected roots

Labelling with WGA–ovomucoid–gold complex was performed on sections corresponding to different stages of root infection.

R. lignosus rhizomorphs contained two types of hyphae: thick-walled hyphae mainly distributed in the outermost part of rhizomorphs [Fig. 2(A)] and thin-walled hyphae mainly localized in close contact with the root surface [Fig. 2(D)]. After incubation of sections showing the host–pathogen interface with the gold-complexed probe, it appeared that fungal walls of both types of hyphae were intensely labelled. Gold particles accumulated preferentially over the internal electron-opaque wall layer of thick-walled hyphae [Fig. 2(B), triple arrowhead; Table 2], whereas they were more unevenly distributed over the intermediate reticulated layer [Fig. 2(B), double arrowhead] and over the external fungal wall layer [Fig. 2(B), arrowhead, Table 2].

Thin walled-hyphae apparently formed a pseudosclerenchymatous structure closely appressed to the root surface [Fig. 2(D), 3(A)]. Gold particles were mainly associated with the innermost wall layer [Fig. 2(C)]. Cytoplasm and organelles, including nucleus and mitochondria, as well as the interhyphal-connecting material [Fig. 2(D), arrowheads] were free of labelling.

Incubation with the WGA–ovomucoid–gold complex showed that labelling was less intense over the wall of the hyphal portion actively involved in dead surface cell wall penetration [Fig. 3(B), arrows; Table 2] than in walls of rhizomorph-included hyphae close to the root surface [Fig. 3(B), double arrowheads; Table 2]. However, numerous gold particles were observed over wall hyphal portions which had penetrated host cells [Fig. 3(B), double arrows].

In phellem cells showing the degradation of the suberized wall, labelling was less intense over wall portions in the channel of fungal penetration [Fig. 3(C) arrowheads; Table 2]. Gold particles were abundant at the tip of penetrating hyphae [Fig. 3(C), double arrowheads]. Variation in the distribution of gold particles was observed within hyphae colonizing phellem cells [Figs 3(C), 4(A), 4(B), 4(C); Table 2]. In altered hyphae, gold particles were found around or inside the fungus [Fig. 4(A)] as well as

layers of fungal walls (arrowheads). Labelling does not occur over external wall layers (double arrowhead). Th, Thick-walled hypha. Bar = 1 µm. (D) Interface between *R. lignosus* rhizomorph (R) and the rubber tree root surface. Note that only thin-walled hyphae (th) are in close contact with external root cells (hc). The interhyphal connecting material (arrowheads) is free of gold labelling. Th, Thick-walled hypha; sw, suberized wall. Bar = 1 µm.
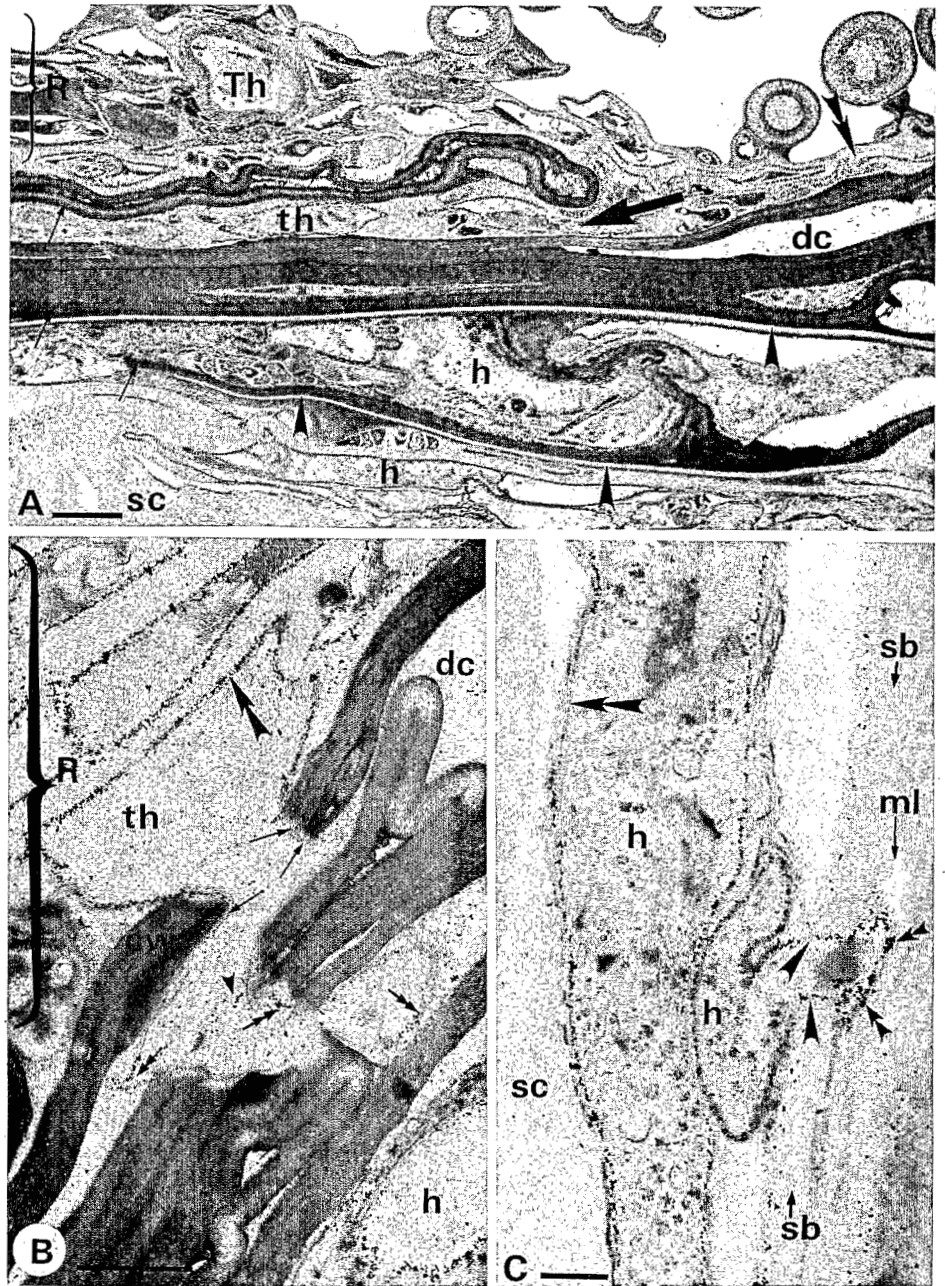
FIG. 3. Transmission electron micrographs of *Rigidoporus lignosus*-infected rubber tree roots double-fixed with glutaraldehyde and osmium tetroxide. Hyphal penetration in roots. Sections were treated with the WGA–ovomucoid–gold complex. (A) Only thin-walled hyphae (th) achieve root invasion (large arrow). Gold particles are absent over host suberized cell walls (arrowheads), host cellulosic cell walls (small arrows), and over the interhyphal connecting material (double arrowhead). dc, Dead cell surface; h, hypha in host cell; R, rhizomorph; sc, suberized cell; Th, thick-walled hypha. Bar = 2 μm. (B) Early stage of root penetration by thin-walled hyphae (th) via wall degradation of dead surface cell (dc). Wall areas of the hypha (h) penetrating host cell
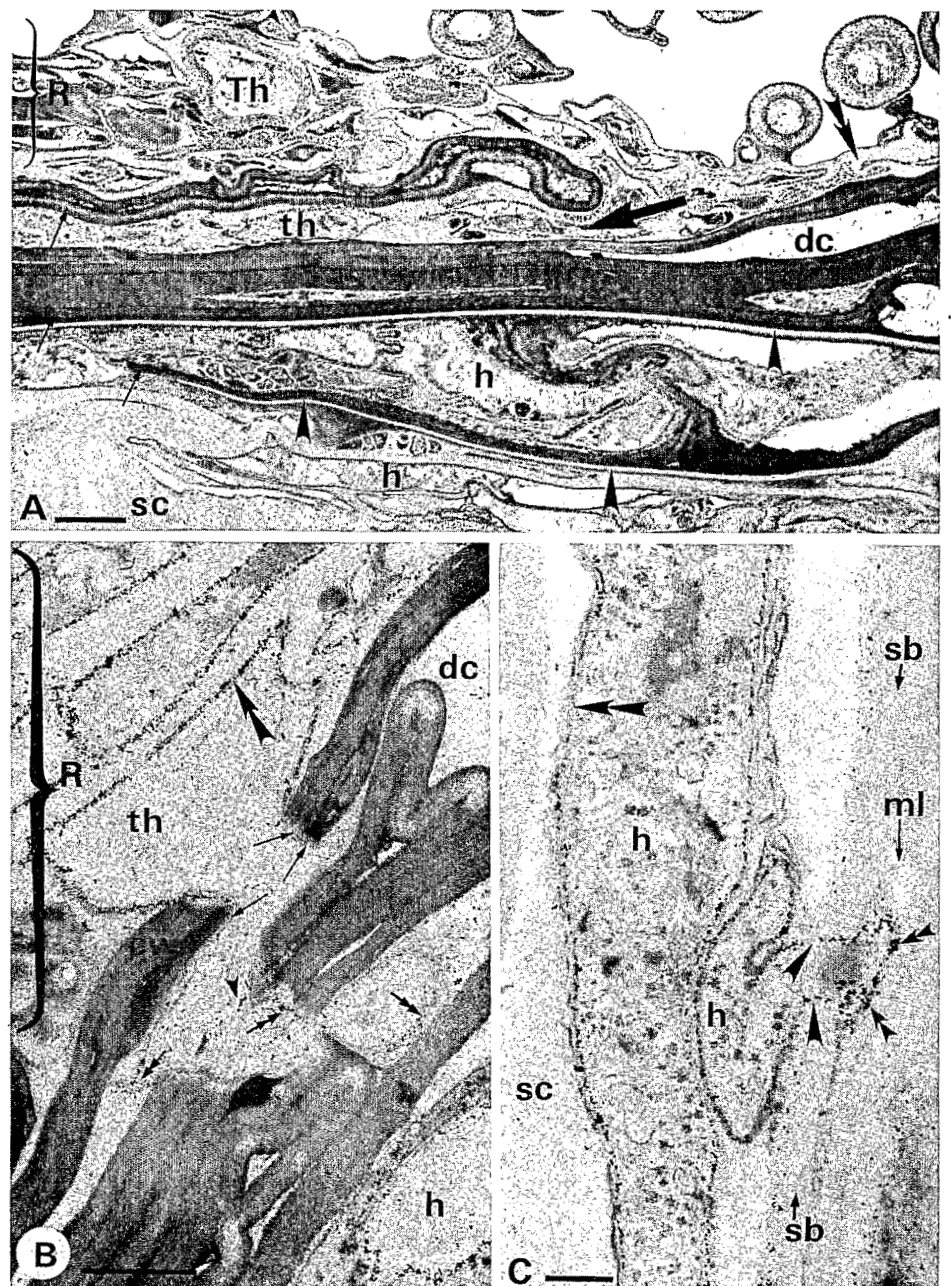
FIG. 3. Transmission electron micrographs of *Rigidoporus lignosus*-infected rubber tree roots double-fixed with glutaraldehyde and osmium tetroxide. Hyphal penetration in roots. Sections were treated with the WGA–ovomucoid–gold complex. (A) Only thin-walled hyphae (th) achieve root invasion (large arrow). Gold particles are absent over host suberized cell walls (arrowheads), host cellulosic cell walls (small arrows), and over the interhyphal connecting material (double arrowhead). dc, Dead cell surface; h, hypha in host cell; R, rhizomorph; sc, suberized cell; Th, thick-walled hypha. Bar = 2 μm. (B) Early stage of root penetration by thin-walled hyphae (th) via wall degradation of dead surface cell (dc). Wall areas of the hypha (h) penetrating host cell

TABLE 2

Density of labelling[a] obtained with WGA–ovomucoid–gold complex over cell walls of Rigidoporus
lignosus *during the infection process*

Fungal localization	Labelling density
Internal layer of thick fungal cell wall in the rhizomorph	$302·85 \pm 115·13$
Medium layer of thick fungal cell wall in the rhizomorph	$103·36 \pm 26·22$
External layer of thick fungal cell wall in the rhizomorph	$106·61 \pm 51·17$
Thin fungal cell walls in the rhizomorph close to the root surface	$2478·08 \pm 365·07$
Fungal cell walls during penetration of dead surface cell walls	$87·94 \pm 58·83$
Intracellular fungal cell walls in phellem cells	$650·02 \pm 99·61$
Fungal cell walls during penetration of phellem cell walls	$398·93 \pm 42·51$
Altered fungal cell wall in phellem cells	$173·72 \pm 69·66$
Intracellular fungal cell walls in xylem elements	$467·69 \pm 99·45$
Fungal cell walls during penetration of xylem cell walls	$66·96 \pm 38·62$
Altered fungal cell wall in xylem elements	$89·27 \pm 39·14$
Fungal sheath	$7·33 \pm 7·96$

[a]Density of labelling is expressed by the number of gold particles $\mu m^{-2} \pm SD$.

in the host cell lumen [Fig. 4(A), 4(B), arrowheads]. The fibrillar material surrounding fungal hyphae in some host cells was slightly labelled [Fig. 4(A), double arrowheads; Table 2]. Wall areas over the subapical region were devoid of gold particles [Fig. 4(C)].

In samples showing infected vascular tissues, the pathogen was seldom observed in phloem cells. The few hyphae that could be found in phloem elements were labelled by a few gold particles after incubation of sections with the WGA–ovomucoid–gold complex (not shown). In contrast, hyphae were abundant in xylem elements. The distribution of gold particles varied within cell walls of hyphae colonizing lignified cells. Gold labelling was frequently intense in walls of intracellular hyphae (Table 2) both in close contact with the host secondary cell walls [Fig 5(A)] and at a distance from the host cell walls [Fig. 5(B)]. At sites of pit penetration [Fig. 5(C) and (D), arrows], only slight gold labelling of fungal walls was noticeable (Table 2), in contrast to the intense labelling observed over walls of the remaining intracellular fungal portion [Fig. 5(D), double arrows; Table 2]. At the apical region of these penetrating hyphae, accumulation of gold particles was apparent [Fig. 5(D), arrowheads].

Changes in wall labelling distribution was also detected in hyphae appressed against the electron-dense material coating pit areas and xylem parenchyma cell walls [Fig. 6(A)]. Very few gold particles were associated with the tip portion [Fig. 6(A),

walls (cw) are free of gold particles (arrows). Portions of hyphal walls remaining in the rhizomorph (R) are heavily labelled (double arrowheads). Gold particles accumulate in localized wall areas (double arrows) of portions of the hypha which has penetrated the root. Note that some gold particles occur in the fungal cytoplasm (arrowhead). Bar = 1 μm. (C) Penetration of suberized wall layers (sb) by *R. lignosus* hyphae (h). Fungal wall as tip appears more labelled (double arrowheads) than lateral walls (arrowheads). Note some areas of intracellular hyphal walls (h) (double arrows) are free of gold particles. Both the unlabelled middle lamella (ml) and unlabelled suberized wall layers (sb) are degraded. sc, Suberized cell. Bar = 0·5 μm.

Benhamou
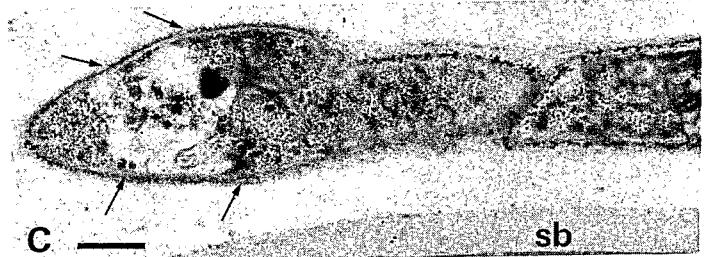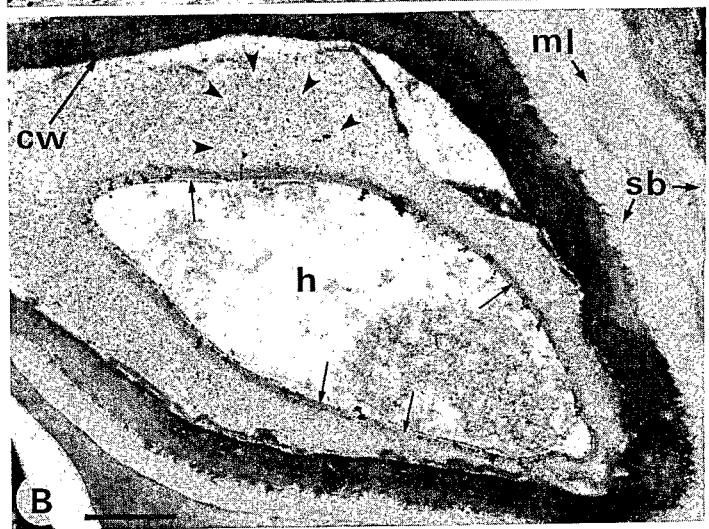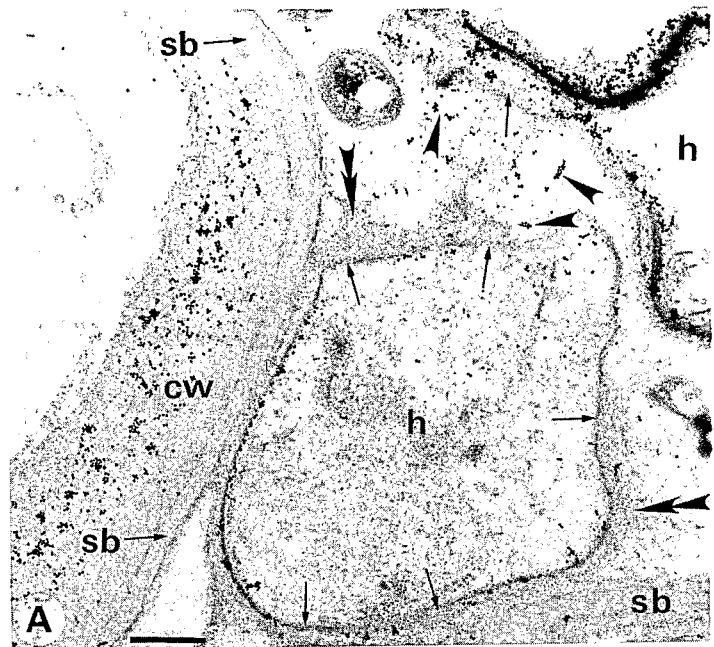
arrowheads], whereas they were more abundant over the remaining part of the fungal wall [Fig. 6(A), arrows].

Observations of sections of slightly decayed roots of rubber tree showed numerous damaged hyphae in xylem cells [Fig. 6(B) and (C)]. Walls of these hyphae were slightly labelled (Table 2). This low labelling occurred in cells showing additional host cell wall layers [Fig. 6(B)] or thin electron-dense deposition along the S3 layer of the secondary wall [Fig. 6(C), arrowheads].

All control tests including incubation of sections with the WGA to which was previously added an excess of N-N'-N''-triacetyl chitotriose, resulted in an absence of labelling over plant secondary walls [Fig. 7(B), Table 3] and over *R. lignosus* hyphal walls [Fig. 7(A), Table 3].

DISCUSSION

The present study indicates that GlcNAc residues are present in both *R. lignosus* hyphal walls and in secondary cell walls of healthy and infected young rubber tree roots. Previous reports demonstrated cytochemically the occurrence of GlcNAc-containing molecules in secondary plant cell walls [5, 9], which are thought to be possibly linked to cell wall lipids [5]. Our results show that GlcNAc-containing molecules also occur in secondary cell walls of the tropical tree, *H. brasiliensis*.

Previous chemical analysis showed that walls of wood decay fungi, including *R. lignosus*, contained large amounts of GlcNAc [11, 22, 28, 42]. In *R. lignosus* rhizomorphs growing on the root surface, gold particles were associated with the walls of both thick- and thin-walled hyphae. Since chitin is a polymer of $\beta(1,4)$-linked GlcNAc residues, it is likely that WGA binding sites are associated with chitin [4]. A quantitative evaluation of the labelling revealed that the intermediate reticulate layer of the thick fungal cell walls was less labelled than the internal layer. This suggests that either low amounts of chitin occur in this layer, or that WGA cannot easily bind to the chitin polymer due to the presence of interfering components. β-Glucans, which are ubiquitous in walls of higher fungi [42], are thought to be covalently cross-linked to chitin in the wall of most basidiomycetes. This chitin–glucan complex contributes wall strength, except in the growing apical region [43]. Assuming that such a complex occurs in the thick-walled hyphae of *R. lignosus*, chitin may not be accessible to the lectin probe.

Infective *R. lignosus* hyphae can revert to a saprophytic state, with accompanying morphogenetic, [7] and biochemical changes [2, 6, 18]. These changes are in-

Fig. 4. Transmission electron micrographs of *Rigidoporus lignosus*-infected rubber tree roots double-fixed with glutaraldehyde and osmium tetroxide. Colonization of phellem cells. Sections were treated with the WGA–ovomucoid–gold complex. (A) Labelling alteration over *R. lignosus* cell walls occurs in well-delineated wall areas (arrows). Numerous gold particles are present in host cell (arrowheads). They are also observed over the fungal cell lumen. The fibrillar matrix surrounding hyphae (double arrowheads) is slightly labelled. Suberized wall layers (sb) are unlabelled, whereas gold particles are abundant over cellulosic wall layers (cw). Bar = 0·5 μm. (B) Labelling of the wall (arrows) of a degenerating hypha localized in phellem cells. Gold particles are released in host cell cytoplasm (arrowheads). Labelling does not occur over the suberized wall layer (sb) or the middle lamella (ml). Note the high electron density of cellulosic wall layers (cw) of the phellem cell. Bar = 0·5 μm. (C) In some hyphae, gold particles are absent over wall areas of the subapical region (arrows). Labelling is regularly distributed over tip walls and other wall areas. sb, Suberized wall layer. Bar = 0·5 μm.
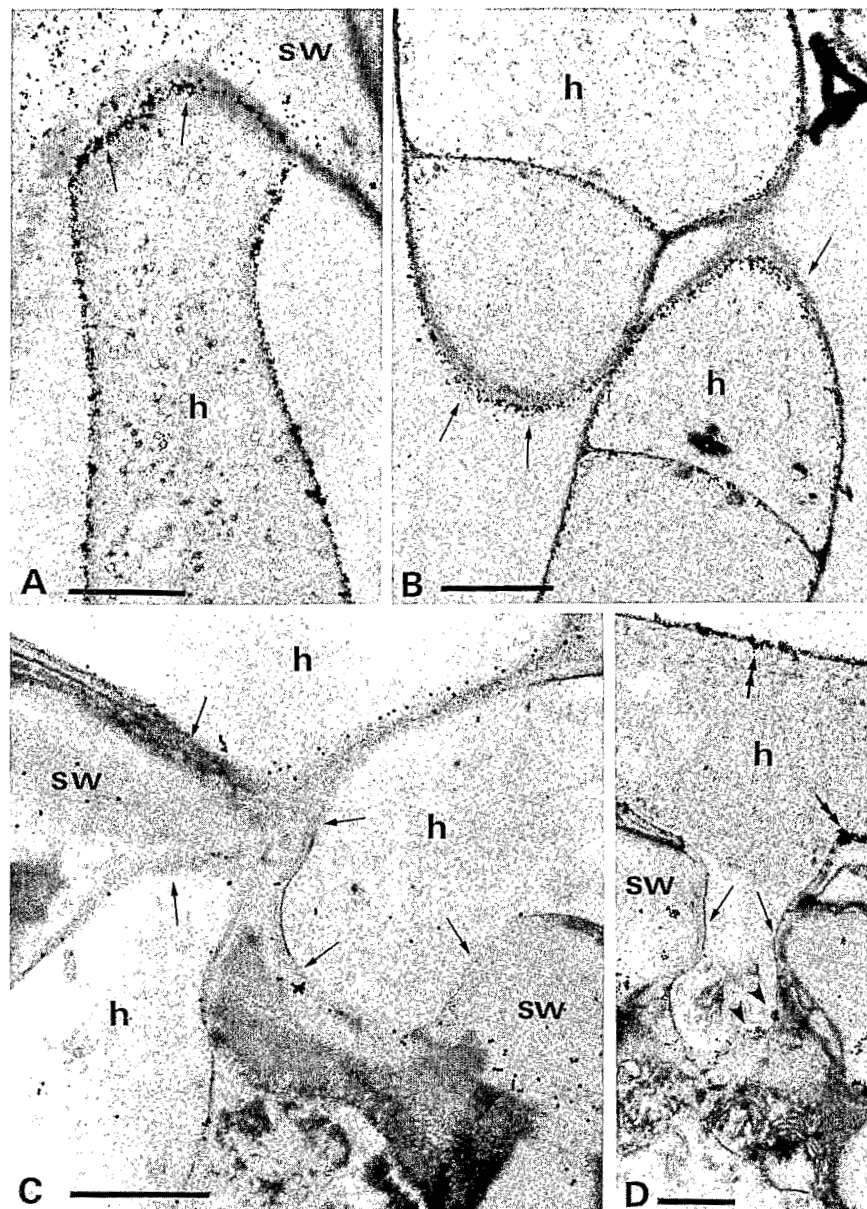
FIG. 5. Transmission electron micrographs of *Rigidoporus lignosus*-infected rubber tree roots double-fixed with glutaraldehyde and osmium tetroxide. Colonization of xylem elements. (A) Sections were treated with the WGA–ovomucoid–gold complex. (A),(B) Distribution of gold particles over hyphal walls localized in lignified cells. *R. lignosus* cell walls are heavily labelled both in close contact (A, arrows) with vessel secondary walls (sw) or at a distance from host cell walls (B, arrows). Bars = 1 μm. (C),(D) Few gold particles are observed over walls (arrows) of branching hyphae (h) during pit penetration by *R. lignosus*. Gold particles are abundant in walls of remaining hyphal portion in the cell lumen (D, double arrows). Note accumulation of gold particles in wall portions of hyphae which have penetrated host cell walls (D, arrowheads). sw, Secondary wall. Bar = 1 μm (C) and 0·4 μm (D).
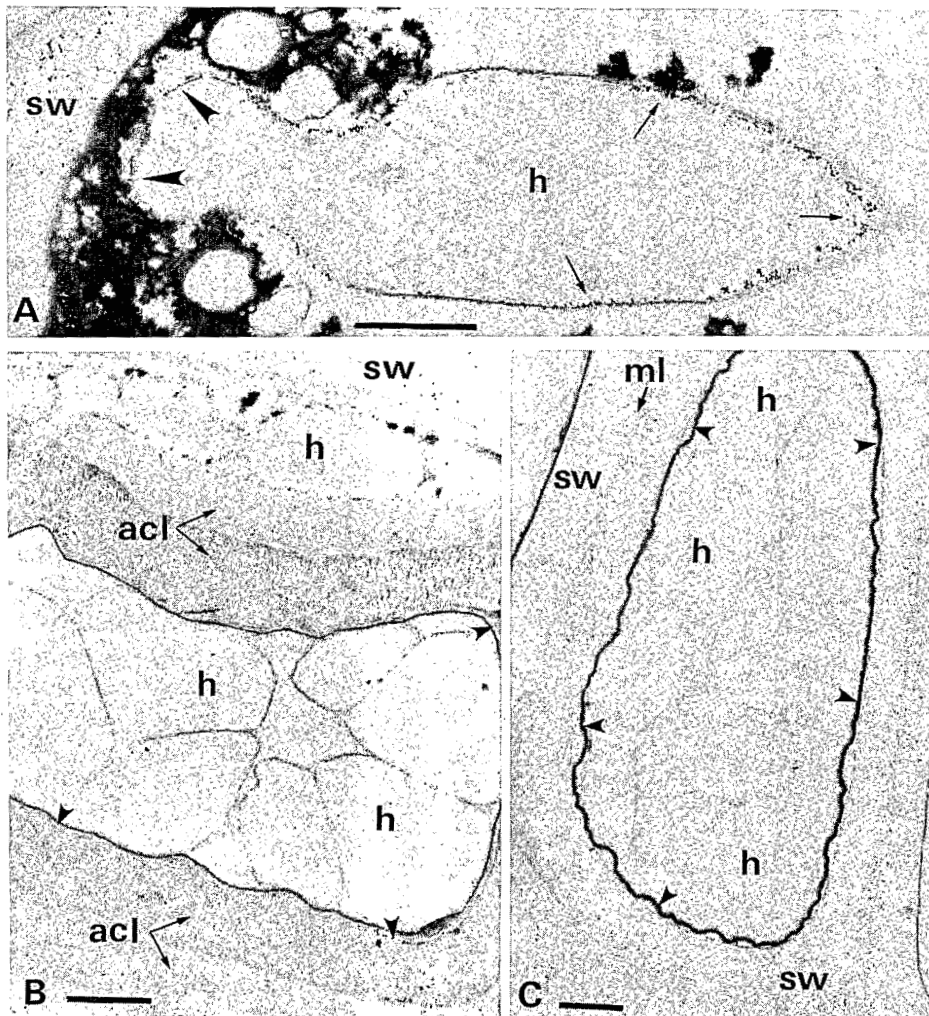
FIG. 6. Transmission electron micrographs of *Rigidoporus lignosus*-infected rubber tree roots double-fixed with glutaraldehyde and osmium tetroxide. Colonization of xylem elements. Sections were treated with the WGA–ovomucoid–gold complex. (A) Differential labelling over walls of hyphal tips (arrowheads) in close contact with electron-dense material localized along secondary walls (sw) of lignified cells. Gold particles are regularly distributed over other wall areas of the hypha (h) (arrows). Bar = 1 µm. (B) Differential labelling over walls of hyphae (h) localized in a xylem fibre showing additional cell wall layers (acl). A thin suberized layer is noticeable along these additional cell layers (arrowheads). sw, Secondary walls. Bar = 1 µm. (C) Differential labelling over walls of hyphae (h) localized in xylem fibres showing electron-dense deposition (arrowheads) along secondary cell walls (sw). Numerous gold particles are distributed over walls of secondary cells. ml, Middle lamella. Bar = 1 µm.

duced by anoxic soil conditions [26]. Since only thin-walled hyphae penetrate the outer root tissue, it is likely that when *R. lignosus* rhizomorphs are infecting the root surface, some thick-walled hyphae undergo pronounced cell wall modifications. A progressive thinning of the reticulated layer of thick fungal cell walls may lead to the
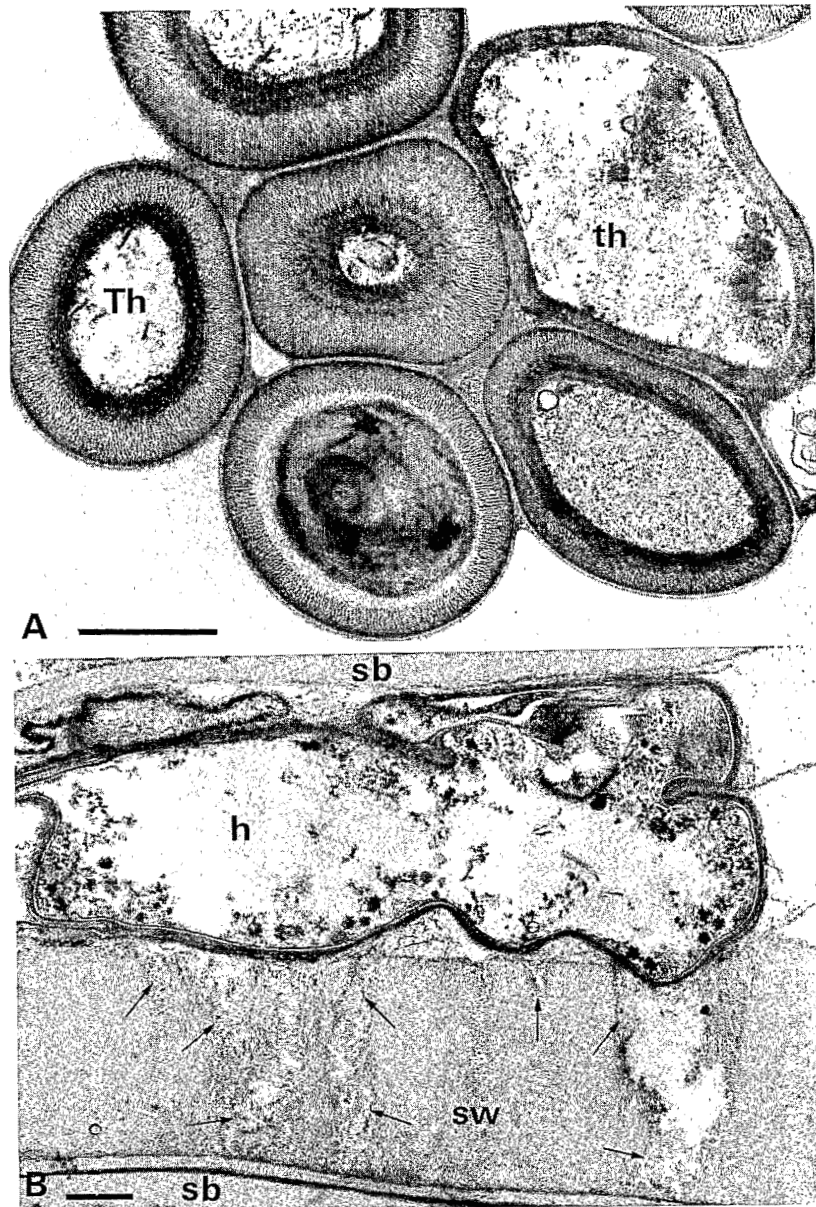
FIG. 7. Control tests. Transmission electron micrographs of *Rigidoporus lignosus*-infected rub
tree roots double-fixed with glutaraldehyde and osmium tetroxide. (A),(B) Preadsorptior
WGA with an excess of *N*-*N'*-*N''*-triacetyl chitrotriose before section labelling results in
absence of gold particles over walls of hyphae (Th, th) in *R. lignosus* rhizomorphs (A) and (
walls of intracellular hyphae (h) in host infected cells (B). Secondary host cell walls (sw) are
free of gold particles (B). Note the intense degradation of host cell walls (arrows). sb, Suber
wall. Bars = 1 μm (A) and 0·5 μm (B).

TABLE 3.

Density of labelling[a] obtained with control tests over host and fungal cell walls

Location	Labelling density
Xylem	$0·71 \pm 1·13$[b]
Phloem	$0·00 \pm 0·00$
Cellulose layer of phellem cell walls	$0·00 \pm 0·00$
Suberized layer of phellem cell walls	$1·36 \pm 2·72$[b]
Dead surface cell walls	$0·00 \pm 0·00$
Intracellular hyphae	$0·00 \pm 0·00$
Thin-walled hyphae in the rhizomorph	$1·57 \pm 3·84$[b]
Thick-walled hyphae in the rhizomorph	$0·13 \pm 0·31$[b]

[a]Density of labelling is expressed by the number of gold particles $\mu m^{-2} \pm SD$.
[b]Some selected areas showed a low background.

formation of thin-walled mycelium with chitin predominantly associated with the inner layers. The thin fungal cell walls are probably more flexible, enabling hyphae to penetrate the roots more easily.

WGA labelling was substantially reduced over the walls of root-penetrating hyphae as compared to that of rhizomorphs. Similarly, reduced labelling was found over walls of branching hyphae responsible for host cell wall penetration. Changes in the amount of chitin in hyphal cell walls during penetration processes suggest the lytic action of fungal host cell wall-degrading enzymes both during the early stage of root penetration [18], and during the process of tissue colonization [17, 19]. Similar changes in the distribution of chitin have also been reported with *Colletotrichum lindemuthianum* when infecting French bean leaf cells (35). Modification or release of chitin from fungal cell walls may, thus, be related to the establishment of root infection, and to colonization.

The release of GlcNAc residues from *R. lignosus* cell walls in the cytoplasm of host infected cells suggests the implication of chitinolytic enzymes in the degradation of fungal cell walls. Forest trees such as oaks [41] and latex-producing plants [24, 25] are known to contain chitinases, enzymes able to hydrolyse fungal chitin [39]. They were extracted from both the phloem of the stem and root. In *H. brasiliensis*, chitinase activity is much higher in the latex of trunks than in leaves of unstressed trees. Moreover, it has been demonstrated that chitinase activity increased in rubber trees both following abiotic stress [23, 24] and *R. lignosus* infection [34]. Thus, our results indicate that *R. lignosus* wall degradation during root colonization of rubber trees, may partially result from a chitinolytic activity expressed not only in laticifers but also in other host cell types.

WGA gold labelling in the host cell indicated the presence of chitin oligomers, since WGA has a high affinity for GlcNAc residues. Chitin oligosaccharides have been successfully assayed for inducing chitinase activity [38] and lignification [1] on other plants. Root rot fungi frequently induce root lignification in infected trees [33]. In infected roots of rubber trees, lignin is a major component of: (i) wall appositions in parenchyma and phellem cells, (ii) additional layers of xylem cell walls as shown in Fig. 6(B), and (iii) compartmentalizing reaction tissue [31]. Moreover, cinnamyl-alcohol

dehydrogenase activity, a key enzyme in lignin monomer biosynthesis, was found to be significantly stimulated in young rubber tree roots after elicitation with *R. lignosus* cell wall extracts [*34*]. Chitin oligosaccharides released from *R. lignosus* into root cells of infected rubber trees may elicit root defence lignification. Lignification has been demonstrated to be an effective response of artificially infected *H. brasiliensis* roots [*33*], preventing subsequent colonization of living tissues and allowing trees to survive.

In conclusion, the present cytochemical investigation provides evidence for changes in the content of chitin in *R. lignosus* cell walls during infection of rubber tree roots. Our observations suggest that changes in the composition of *R. lignosus* cell walls relate to the establishment of infection, and probably with the induction of host defence reactions.

REFERENCES

1. BARBER, M. S., BERTRAM, R. E. & RIDE, J. P. (1989). Chitin oligosaccharides elicit lignification in wounded wheat leaves. *Physiological and Molecular Plant Pathology* **34**, 3–12.
2. BAREYRE, M. J. & BOISSON, C. (1969). Relation entre la morphogénèse de l'appareil végétatif non agrégé de *Leptoporus lignosus* et le métabolisme respiratoire des filaments caractéristiques des deux phases de développement. *Compte rendus de l'Académie des Sciences, Paris Série D* **268**, 2256–2259.
3. BENHAMOU, N. (1988). Ultrastructural localization of carbohydrates on the cell walls of two pathogenic fungi: a comparative study. *Mycologia* **80**, 324–337.
4. BENHAMOU, N. (1989). Preparation and application of lectin–gold complexes. In *Colloidal Gold, Principles, Methods and Applications*, Ed. by M. A. Hayat, Vol. 1, pp. 95–143, Academic Press, New York.
5. BENHAMOU, N. & ASSELIN, A. (1989). Attempted localization of a substrate for chitinases in plant cells reveals abundant *N*-acetyl-D-glucosamine residues in secondary walls. *Biology of the Cell* **67**, 341–350.
6. BENHAMOU, N. & OUELLETTE, G. B. (1986). Ultrastructural localization of glycoconjugates in the fungus. *Ascocalyx abietina*, the scleroderris canker agent of conifers, using lectin–gold complex. *Journal of Histochemistry and Cytochemistry* **34**, 855–867.
7. BOISSON, C. (1968). Mise en évidence de deux phases mycéliennes successives au cours du développement de *Leptoporus lignosus. Compte rendus de l'Académie des Sciences, Paris, Serie D* **274**, 2481–2484.
8. BONFANTE-FASOLO, P., FACCIO, A., PEROTTO, S. & SCHUBERT, A. (1990). Correlation between chitin distribution and cell wall morphology in the mycorrhizal fungus *Glomus versiforme. Mycological Research* **94**, 157–165.
9. CHAMBERLAND, H., CHAREST, P. M., OUELLETTE, G. B. & PAUZÉ, F. J. (1985). Chitinase–gold complex used to localize chitin ultrastructurally in tomato root cells infected by *Fusarium oxysporum* f.sp. *radicis-lycopersici*, compared with a chitin specific gold-conjugated lectin. *Histochemical Journal* **17**, 313–321.
10. CHEE, K. H. (1990). Present status of rubber diseases and their control. *Review of Plant Pathology* **69**, 1423–1430.
11. CHEN, G. C. & JOHNSON, B. R. (1983). Improved colorimetric determination of cell wall chitin in wood decay fungi. *Applied and Environmental Microbiology* **46**, 13–16.
12. CHÉRIF, M. & BENHAMOU, N. (1990). Cytochemical aspects of chitin breakdown during the parasitic action of *Trichoderma* spp. on *Fusarium oxysporum* f.sp. *radicis-lycopersici. Phytopathology* **80**, 1401–1414.
13. DARGENT, R., TOUZÉ-SOULET, J. M. & SAIDALI-SAVY, C. (1989). Mise en évidence de la chitine par le complexe or colloïdal-WGA : différence entre l'apex hyphal et le reste du filament d'*Hypomyces chlorinus* Tul. *Compte rendu de l'Académie des Sciences, Paris, Série D* **308**, 183–188.
14. ESAU, K. (1977). *Anatomy of Seed Plants*, 2nd edition. John Wiley, New York.
15. FRENS, G. (1973). Controlled nucleation for regulation of the particle size in monodisperse gold suspensions. *Nature (Physical Science)* **241**, 20–22.
16. GEIGER, J. P. (1975). Aspects physiologiques et biochimiques de la spécialisation parasitaire. Cas des *Corticium rolfsii* (Sacc.) et *Leptoporus lignosus* (Kl.) Heim ex Patm. Etudes *in vitro. Physiologie Végétale* **14**, 307–330.

7. GEIGER, J. P., HUGUENIN, B., NICOLE, M. & NANDRIS, D. (1986). Laccases of *Rigidoporus lignosus* and *Phellinus noxius*. II. Effects of *R. lignosus* laccase L1 on thioglycolic lignin of *Hevea*. *Applied Biochemistry and Biotechnology* **13**, 97–111.

8. GEIGER, J. P., NICOLE, M., NANDRIS, D. & RIO, B. (1986). Root rot diseases of *Hevea brasiliensis*. I—Physiological and biochemical aspects of root aggression. *European Journal of Forest Pathology* **16**, 22–36.

9. GEIGER, J. P., RIO, B., NICOLE, M. & NANDRIS, D. (1986). Biodegradation of *Hevea brasiliensis* wood by *Rigidoporus lignosus* and *Phellinus noxius*. *European Journal of Forest Pathology* **16**, 147–159.

10. GRANDMAISON, J., BENHAMOU, N., FURLAN, J. & VISSER, S. A. (1988). Ultrastructural localization of *N*-acetylglucosamine residues in the cell wall of *Gigaspora margarita* throughout its life cycle. *Biologie Cellulaire* **63**, 28–30.

11. HEATH, M. C. (1989). *In vitro* formation of haustoria of the cowpea rust fungus, *Uromyces vignae*, in the absence of a living plant cell. I. Light microscopy. *Physiological and Molecular Plant Pathology* **35**, 357–366.

12. JOHNSON, B. R. & CHEN, G. C. (1983). Occurrence and inhibition of chitin in cell walls of wood-decay fungi. *Holzforschung* **37**, 255–259.

13. KUSH, A., GOYVERTS, E., CHYE, M. L. & CHUA, N. H. (1990). Laticifer-specific gene expression in *Hevea brasiliensis*. *Proceedings of the National Academy of Sciences of the U.S.A.* **87**, 1787–1790.

14. MARTIN, M. & GAYNOR, J. J. (1988). Expression of chitinase in latex-producing plants. *Plant Physiology* **86**, S59 (abstract N 354).

15. MARTIN, M. (1991). The latex of *Hevea brasiliensis* contains high levels of both chitinases and chitinases/lysozymes. *Plant Physiology* **95**, 469–476.

16. NANDRIS, D., NICOLE, M. & GEIGER, J. P. (1983). Infections artificielles de jeunes plants d'*Hevea brasiliensis* par *Rigidoporus lignosus* et *Phellinus noxius*. *European Journal of Forest Pathology* **13**, 65–76.

17. NANDRIS, D., NICOLE, M. & GEIGER, J. P. (1987). Root rot diseases of rubber-tree. *Plant Disease* **71**, 298–306.

18. NICOLE, M. (1982). Masse mycélienne et activité laccase au sein des racines d'*Hevea brasiliensis* parasitées par *Rigidoporus lignosus*. *Physiologie Végétale* **20**, 465–475.

19. NICOLE, M. & BENHAMOU, N. (1991). Cytochemical aspects of cellulose breakdown during the infection process of rubber tree roots infected by *Rigidoporus lignosus*. *Phytopathology* **81**, 1412–1420.

20. NICOLE, M., GEIGER, J. P. & NANDRIS, D. (1986). Penetration and degradation of suberized cells of *Hevea brasiliensis* infected with root rot fungi. *Physiological and Molecular Plant Pathology* **28**, 181–185.

21. NICOLE, M., GEIGER, J. P. & NANDRIS, D. (1986). Root rot diseases of *Hevea brasiliensis*. II. Some host reactions. *European Journal of Forest Pathology* **16**, 37–55.

22. NICOLE, M., GEIGER, J. P. & NANDRIS, D. (1987). Ultrastructural aspects of rubber tree root rot diseases. *European Journal of Forest Pathology* **17**, 1–10.

23. NICOLE, M., GEIGER, J. P. & NANDRIS, D. (1991). Defense mechanisms of root trees in angiosperms to fungal invasion. In *Defense Mechanisms of Woody Plants against Fungi*, Ed. by R. A. Blanchette & A. R. Biggs, Springer Verlag, Berlin, (in press).

24. NICOLE, M., TOPPAN, A., GEIGER, J. P., ROBY, D., NANDRIS, D. & RIO, B. (1991). Defense responses of *Hevea brasiliensis* to elicitors from root rot fungi. *Canadian Journal of Botany* **69**, 1819–1824.

35. O'CONNELL, R. J. & RIDE, J. P. (1990). Chemical detection and ultrastructural localization of chitin in cell walls of *Colletotrichum lindemuthianum*. *Physiological and Molecular Plant Pathology* **37**, 39–53.

36. RAIKHEL, N. V., MISHKIND, M. & PALEVITZ, B. A. (1984). Immunocytochemistry in plants with colloidal gold conjugates. *Protoplasma* **121**, 25–33.

37. RIDE, J. P. & DRYSDALE, R. B. (1975). A chemical method for estimating *Fusarium oxysporum* f.sp. *lycopersici* in infected tomato plants. *Physiological Plant Pathology* **1**, 409–420.

38. ROBY, D., GADELLE, A. & TOPPAN, A. (1987). Chitin oligosaccharides as elicitors of chitinase activity in melon plants. *Biochemical and Biophysical Research Communications* **143**, 885–892.

39. SCHLUMBAUM, A., MAUSCH, F., VÖGELI, U. & BOLLER, T. (1986). Plant chitinases are potent inhibitors of fungal growth. *Nature* **324**, 365–367.

40. TOPPAN, A. & ESQUERRÉ-TUGAYÉ, M. T. (1976). An improved approach for the accurate determination of fungal pathogens in diseased plants. *Physiological Plant Pathology* **9**, 241–251.

41. WARGO, P. M. (1975). Lysis of the cell wall of *Armillaria mellea* by enzymes from forest trees. *Physiological Plant Pathology* **5**, 99–105.

42. WESSELS, J. G. H. (1987). Growth and development in a model basidiomycete: *Schizophyllum commune*. In. *Lignin Enzymatic and Microbial Degradation*, Les colloques de l'INRA **40**, 19–42.

43. WESSELS, J. G. H., SIETSMA, J. H. & SONNENBERG, A. S. M. (1983). Wall synthesis and assembly during hyphal morphogenesis in *Schizophyllum commune*. *Journal of General Microbiology* **129**, 1607–1616.